Test-particle simulations of collisional impurity transport in rotating spherical tokamak plasmas

R. J. McKay[1], K. G. McClements[2], A. Thyagaraja[2], L. Fletcher[1]

[1] *University of Glasgow, Department of Physics and Astronomy, Glasgow, G12 8QQ, UK*

[2] *EURATOM/UKAEA Fusion Association, Culham Science Centre, Abingdon, Oxfordshire, OX14 3DB, United Kingdom*

Abstract

A full orbit test-particle approach is used to study the collisional transport of impurity (carbon) ions in spherical tokamak (ST) plasmas with transonic and subsonic toroidal flows. The efficacy of this approach is demonstrated by reproducing the results of classical transport theory in the large aspect ratio limit. The equilibrium parameters used in the ST modelling are similar to those of plasmas in the MAST experiment. The effects on impurity ion confinement of both counter-current and co-current rotation are determined. Various majority ion density and temperature profiles, approximating measured profiles in rotating and non-rotating MAST plasmas, are used in the modelling. It is shown that transonic rotation (both counter-current and co-current) has the effect of reducing substantially the confinement time of the impurity ions. This effect arises primarily because the impurity ions, displaced by the centrifugal force to the low field region of the tokamak, are subject to a collisional diffusivity that is greater than the flux surface-averaged value of this quantity (Helander 1998 *Phys. Plasmas* **5**, 1209). For a given set of plasma profiles, the ions are found to be significantly less well-confined in co-rotating plasmas than in counter-rotating plasmas. The poloidal distribution of losses exhibits a pronounced up/down asymmetry that is consistent with the direction of the net vertical drift of the impurity ions.

1. Introduction

The use of high power tangential neutral beam injection (NBI) to deliver heat and angular momentum to plasmas in the MAST spherical tokamak [1] has resulted in toroidal rotation velocities in excess of the sound speed in the plasma core [2]. The beamline geometry in MAST is fixed, but the direction of the plasma current I_p can

be reversed so that the ions (deuterons) in a given beamline are born with toroidal velocity components in the counter-I_p direction rather than the more usual co-current direction. Despite the fact that a high proportion of beam ions are promptly lost in such cases, the use of counter-current NBI in MAST has produced high performance discharges, with energy confinement times greater than those achieved with co-current beam injection [2]. Bulk plasma toroidal rotation velocities in counter-NBI MAST plasmas are typically higher than those in plasmas with co-current injection. Losses of counter-injected beam ions induce an inward-directed radial bulk ion return current, and hence a torque in the counter-current direction, which spins the plasma up to sonic Mach numbers M of order unity [3, 4, 5]. There is evidence that the improvement in energy confinement brought about by reversing the beam injection direction in MAST can be attributed to micro-turbulence suppression due to radial shear in the toroidal flow [2]. Toroidal rotation in tokamaks can also be beneficial in terms of suppressing magnetohydrodynamic (MHD) instabilities, including sawtooth oscillations [6], neoclassical tearing modes [7], and resistive wall modes [8].

Although rotating plasmas have attractive features with regard to the possibility of micro-turbulence suppression and MHD stability, the irreducible transport arising from particle collisions (i.e. neoclassical transport) can be enhanced rather than diminished by the presence of toroidal flow. For banana regime ions in a pure large aspect ratio plasma, Hinton and Wong [9] showed that rotation increases the neoclassical thermal conductivity by a factor $1 + \mathcal{O}(M^2)$. This analysis was subsequently extended to the case of an impure large aspect ratio plasma by Wong [10], who showed that the neoclassical transport coefficients of impurity ions are also enhanced in the banana regime. In general it is desirable that impurity ions, specifically, are transported rapidly out of a burning plasma, since they dilute the fusion fuel.

Helander [11] pointed out a hitherto-neglected mechanism whereby rotation could increase neoclassical transport, arising from the fact that the centrifugal force in a spinning plasma causes heavy impurity ions to accumulate on the low magnetic field side of each flux surface. This effect, observed experimentally using soft X-ray tomography in ASDEX [12] and JET [13], and reconsidered theoretically by Wesson [14], causes neoclassical particle diffusivities to be enhanced, since they scale inversely with the square of the field. In the case of ASDEX the measured impurity density also exhibited a substantial up/down asymmetry in the grad-B and centrifugal drift directions [12]. Hsu and Sigmar [15] considered the Pfirsch-Schlüter regime in a strongly rotating plasma and showed that up/down impurity density asymmetry can be driven by parallel (to the magnetic field) friction between bulk and impurity ions. Fülöp and Helander [16] examined neoclassical transport in rotating impure plasmas with steep temperature and density profiles, and found that the impurities can accumulate on the *inboard* (high field) side of a flux surface if the gradients are sufficiently large. Recently, Newton and Helander [17] have demonstrated that the poloidal redistribution of impurity ions in a rotating plasma can increase significantly neoclassical momentum transport.

In view of the substantial body of literature on collisional transport in rotating impure tokamak plasmas, it is worthwhile adopting a direct numerical approach to this problem. To this end we use a test-particle full orbit code `CUEBIT` [18] to study the transport of carbon impurity ions in collisional MAST-like plasmas with and without toroidal flows. The Monte Carlo test-particle method provides an alternative to the usual approach based on the drift kinetic equation: it does not, of course, yield analytical results, but it has the considerable advantage of requiring no approximations to be made apart from the test-particle assumption. Thus, the collisionality regime of the trace minority ions, the profiles of the bulk plasma particles with which they are colliding, and the equilibrium magnetic configuration, can all be prescribed arbitrarily. Like experiments, test-particle simulations can yield unanticipated results that stimulate further, analytical, investigation.

The rest of the paper is structured as follows. In Section 2 we describe the model employed to investigate test particle transport in stationary and rotating MAST-like plasmas, and how we incorporate collisions within the framework of our orbit code. In Section 3 we present the results of our simulations. In Section 4 we draw some conclusions, discuss their implications, and suggest possibilities for future investigation.

2. Model

2.1. Equilibrium

The presence of transonic toroidal flows means that the inertial and pressure gradient terms in the MHD momentum balance equation are *ipso facto* of comparable magnitude, and the Grad-Shafranov equation determining the equilibrium poloidal flux Ψ must be generalised to describe such flows [19]. Savenko *et al* [20] solved this generalised equation numerically for a set of MAST-like equilibria with essentially identical boundaries and toroidal Mach numbers in the plasma core M_φ ranging from zero up to and exceeding unity. It was found that the rotation produced an outward shift of the magnetic flux surfaces inside the plasma, although the shift was small: less than 4cm (around 6% of the plasma minor radius) at the magnetic axis for $M_\varphi = 1$. For simplicity, we neglect the relatively small effect of transonic toroidal flows on flux surfaces and use the same equilibrium for the stationary and rotating cases. Specifically, we use the following solution of the Grad-Shafranov equation for stationary plasma equilibria [21, 22]:

$$\Psi(R,Z) = \Psi_0 \left\{ \frac{\gamma}{8} \left[(R^2 - R_0^2)^2 - R_b^4 \right] + \frac{1-\gamma}{2} R^2 Z^2 \right\}, \tag{1}$$

where R and Z denote distance from the tokamak symmetry axis and vertical distance from the midplane, and Ψ_0, γ, R_0 and R_b are positive constants. The plasma boundary is defined by $\Psi = 0$. If the plasma current is taken to be in the negative φ direction

then Ψ_0 is positive and $\Psi \leq 0$ throughout the plasma. The poloidal flux Ψ is defined such that

$$\mathbf{B} = -\frac{1}{R}\frac{\partial \Psi}{\partial Z}\mathbf{e}_R + B_\varphi \mathbf{e}_\varphi + \frac{1}{R}\frac{\partial \Psi}{\partial R}\mathbf{e}_Z, \tag{2}$$

where B_φ is the toroidal field and $\mathbf{e}_R$, $\mathbf{e}_\varphi$, $\mathbf{e}_Z$ are unit vectors in a right-handed (R,φ,Z) coordinate system, with φ denoting toroidal angle. Equation (2) is a solution of the Grad-Shafranov equation if RB_φ is constant, which we assume, for simplicity, throughout this paper.

Although, as noted above, the effects of even transonic toroidal flows on flux surfaces are fairly modest when the plasma boundary is held fixed, force balance in the bulk ion and electron fluids requires the presence of an electric field which must be taken into account when computing particle trajectories. Taking the limit of vanishing electron mass, and assuming that electron temperature T_e and ion temperature T_i are both flux functions, Thyagaraja and McClements [23] showed that the electrostatic potential associated with purely toroidal rotation in a two-fluid plasma (i.e. a plasma with only trace quantities of impurity ions) is given by

$$\Phi = \Phi_0(\Psi) + \frac{m_i T_e \Omega^2 R^2}{2e(T_e + T_i)}, \tag{3}$$

where e is proton charge, Φ_0 is a flux function, m_i is bulk ion mass, and Ω is the toroidal rotation rate. It is straightforward to show that in the ideal MHD limit

$$\Phi = \Omega\Psi, \tag{4}$$

indicating that Ω is then a flux function. Comparing equations (3) and (4), we identify Φ_0 with $\Omega\Psi$. The second term on the right hand side of equation (3), which can be regarded as a non-ideal correction term, is required in order to maintain quasi-neutrality when, as a consequence of the centrifugal force associated with toroidal rotation, the electron and ion densities are not constant on a given flux surface [14]. Despite the fact that this term is invariably much smaller than the first term under tokamak conditions, it is essential to take it into account since it is not a flux function. The electric field $\mathbf{E} = -\nabla\Phi$ is therefore not purely radial, and the associated $\mathbf{E} \times \mathbf{B}$ drift does not lie in the flux surface. This correction to the electric field produces a force in the inward major radial direction, thereby reducing the effect of the centrifugal force. Indeed, since the major radial component of the electric field is

$$E_R = -\frac{\partial \Phi}{\partial R} = -\Omega R B_Z - \frac{T_e}{T_i + T_e}\frac{m_i \Omega^2 R}{e}. \tag{5}$$

it follows that for the case of fully ionised impurities ($Z/A \simeq 1/2$ where Z, A denote impurity ion charge state and mass number) in deuterium plasmas with $T_i \simeq T_e$, the electric force associated with the ideal MHD-violating part of equation (4) is approximately equal to one half of the centrifugal force $m_Z \Omega^2 R$ on co-rotating impurity

ions of mass m_Z. Wesson [14] showed that for a trace impurity species in a plasma with singly-charged bulk ions, the density distribution on a given flux surface is of the form

$$n_Z = n_{Z0} \exp\left[\left(1 - \frac{T_e}{T_i + T_e} Z \frac{m_i}{m_Z}\right) \frac{m_Z \Omega^2 R^2}{2T_Z}\right], \tag{6}$$

where T_Z is impurity ion temperature and n_{Z0} is a constant for the flux surface in question; the impurity ion distribution across the entire plasma cross-section can be modelled using this expression if n_{Z0} is taken to be a flux function.

For the purpose of computing impurity ion trajectories we also take into account the presence of a toroidal electric field associated with the plasma loop voltage. This field crosses on the poloidal magnetic field to give an inward-pointing $\mathbf{E} \times \mathbf{B}$ flow that causes impurity accumulation in the plasma core even without rotation (the "Ware pinch" effect) [24]. It is sufficient for our purposes to include a constant toroidal electric field directed in the plasma current direction, i.e. the negative φ direction. Under steady-state conditions the loop voltage V in MAST is typically a few volts [25]: we set $E_\varphi = V/2\pi R = 0.3\mathrm{Vm}^{-1}$.

2.2. Treatment of collisions

`CUEBIT` is used to solve the Lorentz force equation for charged particles in arbitrary electric and magnetic fields using an algorithm that ensures conservation of kinetic energy to machine accuracy when $\mathbf{E} = \mathbf{0}$ [18]. For the case in which $\mathbf{E}$ is a finite potential field, the total energy of collisionless particles is generally conserved to a satisfactory level of accuracy by taking the timestep to be around a tenth of a Larmor period of less.

The code can be extended in a straightforward way to include Coulomb collisions in a rotating plasma by adding to the Lorentz force a drag term, resulting from collisions with bulk ions whose average toroidal velocity v_φ is nonzero, and a noise term that ensures relaxation of the test particle population to a (co-rotating) Maxwellian distribution whose temperature T is equal to that of the bulk ions. In the laboratory frame the Lorentz force equation then takes the form

$$m_Z \frac{d\mathbf{v}}{dt} = Ze(\mathbf{E} + \mathbf{v} \times \mathbf{B}) - \frac{m_Z}{\tau}(\mathbf{v} - v_\varphi \mathbf{e}_\varphi) + m_Z \mathbf{r}(t). \tag{7}$$

Here τ is a prescribed collision time (assumed to be velocity-independent) and $\mathbf{r} = (r_x, r_y, r_z)$ is a set of random numbers, chosen independently for each particle and at each time step, with zero mean and variance

$$\sigma^2 = \frac{u_i^2}{\tau \Delta t}, \tag{8}$$

where $u_i = (2T/m_Z)^{1/2}$ is the desired test particle thermal speed and Δt is the time step used in the code [26]. For simplicity we assume that the entire bulk plasma is rotating

as a single rigid body, so that $\Omega = v_\varphi/R$ is a constant. For the case of counter-current rotation, produced in MAST by counter-current neutral beam injection, $v_\varphi > 0$. The drag term on the right-hand side of equation (8) ensures that after a sufficiently long time the minority ions acquire the same mean flow velocity as the bulk ions with which they are colliding, i.e. $v_\varphi \mathbf{e}_\varphi$. We neglect collisions of the test particles with electrons and beam ions.

For the usual case of a Maxwellian distribution of field particles the collision time τ is given by the expression [27]

$$\frac{1}{\tau} = \left(1 + \frac{m_Z}{m_i}\right) \psi(x) \nu_0, \tag{9}$$

where $x = m_i v^2/2T$, v being the test particle speed, the function ψ is given by

$$\psi(x) = \frac{2}{\sqrt{\pi}} \int_0^x t^{1/2} e^{-t} dt, \tag{10}$$

and for singly-ionised field particles of density n

$$\nu_0 = \frac{Z^2 e^4 n \ln \Lambda}{4\pi \epsilon_0^2 m_Z^2 v^3}, \tag{11}$$

where ϵ_0 is the permittivity of free space and $\ln \Lambda$ is the Coulomb logarithm. We assume that the test particle mass m_Z is large compared with the bulk ion mass m_i; if the test particles are Maxwellian-distributed with temperature T, we can then take the limit $x \ll 1$, in which case

$$\psi \simeq \frac{4}{3\sqrt{\pi}} \left(\frac{m_i}{2T}\right)^{3/2} v^3, \tag{12}$$

and equation (10) reduces to

$$\frac{1}{\tau} = \frac{m_i^{1/2}}{m_Z} \frac{Z^2 e^4 n \ln \Lambda}{6\sqrt{2}\pi^{3/2} \epsilon_0^2 T^{3/2}}. \tag{13}$$

The radial profiles of n and T, upon which this collision rate depends, will be specified in section 3.2.

3. Test Particle Simulations

3.1. Benchmarking orbit code at large aspect ratio

Before investigating the collisional transport of impurity ions in a rotating spherical tokamak, we test the collisional version of `CUEBIT` by applying it to test particles

in a non-rotating, large aspect ratio tokamak with circular flux surfaces, assuming a constant specified collision time and $\mathbf{E} = \mathbf{0}$, and comparing the output to a particular analytic solution of the transport problem. For this purpose we use the following expression for the poloidal flux:

$$\Psi = \frac{\mu_0 R_0 I_p}{4\pi a^2} \left[(R - R_0)^2 + Z^2 \right], \tag{14}$$

where μ_0 is the permeability of free space, R_0 is the major radius of the magnetic axis, a is minor radius and I_p is plasma current. We again take $RB_\varphi \equiv R_0 B_0$ to be a constant.

The analytic solution is arrived at as follows: the cross-field diffusivity of particles undergoing classical transport is given by (see e.g. [28])

$$D_\perp \sim \frac{\rho^2}{\tau}, \tag{15}$$

where $\rho = (T/m_Z)^{1/2} m_Z/ZeB$ is the typical ion Larmor radius. This result can be obtained using a simple random walk argument. By definition, τ is the time taken for a particle to be deflected by a large angle due to collisions: when such a deflection occurs, it is evident that the particle's guiding centre can move across the magnetic field by a distance of order ρ. The relation given by equation (15) between step length ρ, collision time τ and diffusivity $D_\perp$ then follows from an argument first used by Einstein [29] in a discussion of Brownian motion, but applicable (with appropriate modifications) to particle diffusion in magnetised plasmas. In toroidal plasmas of finite aspect ratio $A = R_0/a$, the diffusivity is of course enhanced by neoclassical effects, but equation (15) is applicable to test particles undergoing purely collisional transport in the limit $A \to \infty$. Taking $D_\perp$ to be constant, and neglecting sources and sinks, the temporal evolution of the test particle density n_Z is then given by a simple diffusion equation of the form

$$\frac{\partial n_Z}{\partial t} = \nabla \cdot (D_\perp \nabla n_Z) = \frac{D_\perp}{r} \frac{\partial}{\partial r} \left(r \frac{\partial n_Z}{\partial r} \right), \tag{16}$$

where $r = [(R - R_0)^2 + Z^2]^{1/2}$ is minor radial distance from the magnetic axis at $R = R_0$, $Z = 0$. Solutions of this equation satisfying the boundary condition $n_Z(a) = 0$ can be expressed as Fourier-Bessel series of the form [30]

$$n_Z(r, t) = \sum_{i=1}^{\infty} n_{0i} \exp\left(-\gamma_i^2 D_\perp t/a^2 \right) J_0 \left(\gamma_i \frac{r}{a} \right), \tag{17}$$

where γ_i is the i-th positive zero of J_0, the Bessel function of order zero. Setting $t = 0$ in this result, multiplying by $xJ_0(\gamma_j x)$ where $x = r/a$, integrating with respect to x, and making use of the orthogonality relation [31]

$$\int_0^1 x J_0(\gamma_j x) J_0(\gamma_i x) dx = \frac{1}{2} J_1^2(\gamma_j) \delta_{ij}, \tag{18}$$

where δ_{ij} is the Kronecker delta symbol, we deduce that the coefficients in equation (17) are given by

$$n_{0i} = \frac{2}{J_1^2(\gamma_i)} \int_0^1 x J_0(\gamma_i x) n_z(ax, 0) dx. \tag{19}$$

We can evaluate these coefficients for the case in which all the minority ions initially lie at the magnetic axis. Denoting by N_0 the total number of minority ions initially in the system, we then have

$$n_Z(r, 0) = \frac{N_0 \delta(r)}{2\pi^2 R_0 r}, \tag{20}$$

where δ is the Dirac delta function. Equation (17) then has the explicit form

$$n_Z(r, t) = \frac{N_0}{2\pi^2 R_0 a^2} \sum_{i=1}^{\infty} \frac{J_0(\gamma_i r/a)}{J_1^2(\gamma_i) \exp(\gamma_i^2 D_\perp t/a^2)}. \tag{21}$$

After a few collisional diffusion times only the $J_0(\gamma_1 r/a)$ term in this expansion will contribute significantly, and n_Z then decays in a purely exponential fashion, the associated confinement time being $\tau_c = a^2/\gamma_1^2 D_\perp \simeq 0.17(a^2/\rho^2)\tau$. In setting $n_Z = 0$ at $r = a$ we have effectively assumed that the diffusion rate outside this radius is infinite. This can be simulated in `CUEBIT` by removing a particle permanently from the system as soon as it crosses the plasma boundary.

In order to compare the predictions of classical transport theory with results from `CUEBIT` in a way that minimises statistical noise in the latter, we compute the temporal evolution of the total number of particles remaining in the system, $N(t)$:

$$N(t) = 4\pi^2 R_0 \int_0^a r n_Z(r, t) dr. \tag{22}$$

Making use of the identity

$$\frac{d}{dx}(x J_1(x)) = x J_0(x), \tag{23}$$

we deduce that

$$N(t) = 2N_0 \sum_{i=1}^{\infty} \frac{\exp[-\gamma_i^2 D_\perp t/a^2]}{\gamma_i J_1(\gamma_i)}. \tag{24}$$

The assumption of uniform $D_\perp$ used to derive this result requires in general that T, B and τ do not vary across the plasma. We can prescribe constant T and τ in the collisional terms in equation (7), but spatial variations in B are unavoidable in a tokamak of finite aspect ratio. To minimise these variations we set $a = 1$m and $R_0 = 10^2$m, giving an aspect ratio $A = 10^2$. The toroidal field B_0 was set equal to 3T, and the plasma current $I_p = 30$kA, giving a safety factor at the plasma edge $q \simeq 2\pi a^2 B_0/\mu_0 R_0 I_p \simeq 5$. An artificially low value was adopted for the collision time in order to minimise the impact of modifications to purely classical transport arising from drift orbit effects: τ was set equal to 10^{-6}s . This is still much longer than the particle cyclotron period (~ 40ns). A total of 10^4 fully ionised carbon ions (C^{6+}) were

launched from the magnetic axis at $t = 0$ with a Maxwellian velocity distribution at $T = 100$ eV. The temperature specified in the variance of the noise terms in equation (7) was 1 keV. The bulk ions were assumed to have zero net toroidal rotation, i.e. v_φ was set equal to zero. After a few tens of collision times it was found that the effective temperature of the C^{6+} population had increased to a value very close to 1 keV.

The dashed curve in Figure 1 shows the temporal evolution of the number of simulated C^{6+} ions remaining in the plasma. The solid curve in this figure shows $N(t)$ computed using equation (24). It can be seen that the theoretical prediction represented by equation (24) is in excellent agreement with the particle simulation results: the two curves deviate from each other by around 1% at most, which is consistent with the expected level of statistical noise in a simulation with 10^4 particles.

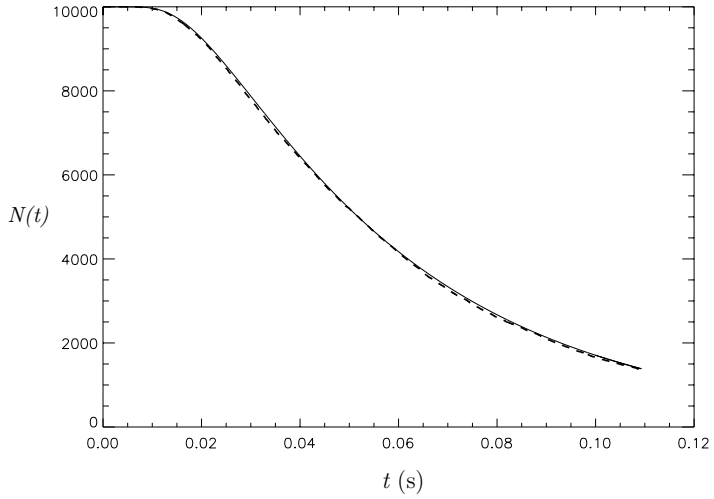

Figure 1: Computed $N(t)$ obtained using `CUEBIT` (dashed curve) and equation (24) (solid curve) for tokamak with aspect ratio $R_0/a = 10^2$. The collision time was set equal to $\tau = 10^{-6}$s and 10^4 particles were used in the simulation.

When the collision time is increased to 10^{-5}s we find that the particle confinement time inferred from `CUEBIT` is significantly shorter than the classical prediction (see figure 2). The model used to derive equation (24) is based on the premise that particles can only be transported across the magnetic field by collisions, whereas particles simulated using `CUEBIT` undergo grad-B and curvature drifts in any tokamak equilibrium with finite aspect ratio, however large. Figure 2 indicates that drifts can cause the transport of test particles to be enhanced above the classical level even when, as in this case, the particles lie well within the Pfirsch-Schlüter regime throughout the plasma and the tokamak aspect ratio is much larger than unity.

We carried out a second set of simulations with aspect ratio $A = 10^4$ ($R_0 = 10^4$m, $a = 1$m) and very low current ($I_p = 1$A), thereby ensuring that the magnetic field was very nearly straight and uniform throughout the plasma. The other parameters were identical to those used previously, with collision times of 10^{-5}s and 10^{-4}s. Results obtained with the shorter value of τ are shown in figure 3; it is clear that once again

there is very good agreement between theory and simulation. The difference between the two curves arising from statistical noise is somewhat greater than that in figure 1 due to the fact that fewer particles were used in the simulation. A similar level of agreement was found in the simulation with $\tau = 10^{-4}$s. We have thus demonstrated that the scheme used to represent collisions in `CUEBIT` leads to classical transport in the appropriate limit, and can be applied with confidence to realistic tokamak scenarios.

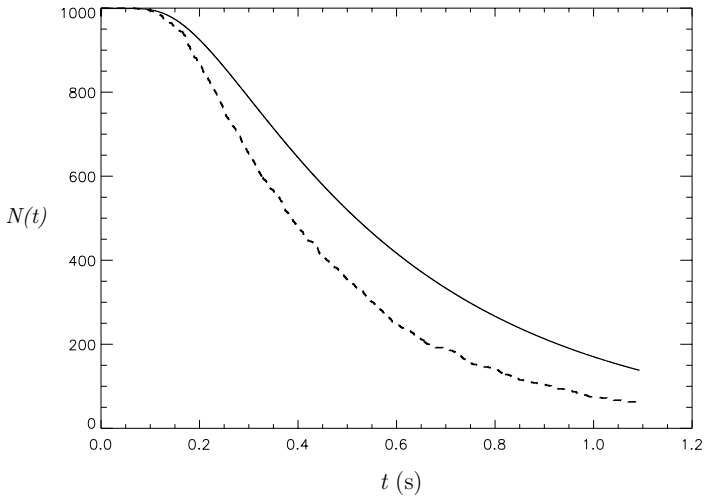

Figure 2: Computed $N(t)$ obtained using `CUEBIT` (dashed curve) and equation (24) (solid curve) for tokamak with aspect ratio $R_0/a = 10^2$. The collision time was set equal to $\tau = 10^{-5}$s and 10^3 particles were used in the simulation.

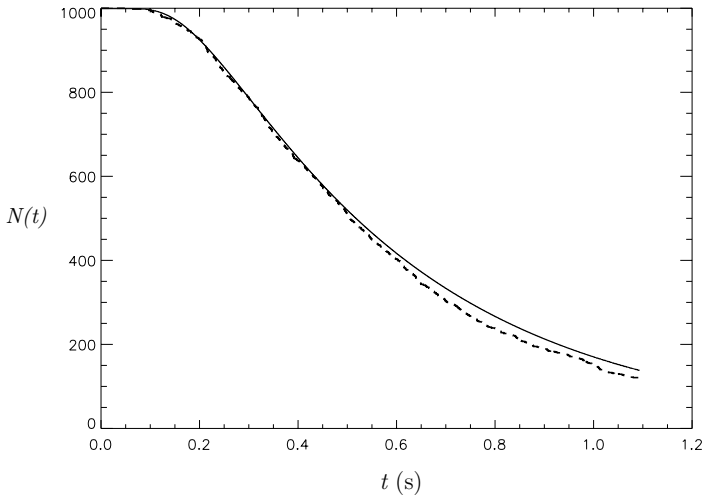

Figure 3: Computed $N(t)$ obtained using `CUEBIT` (dashed curve) and equation (24) (solid curve) for tokamak with aspect ratio $R_0/a = 10^4$. The collision time was set equal to $\tau = 10^{-5}$s and 10^3 particles were used in the simulation.

3.2. MAST simulation parameters

Unless otherwise specified, the parameters used in our MAST simulations are those listed in Table 1. We computed the orbits of test particle carbon impurity ions for three particular scenarios: $\Omega = 0$, $\Omega = 2 \times 10^5$ rad s^{-1} (counter-current rotation) and $\Omega = -2 \times 10^5$ rad s^{-1} (co-current rotation). The bulk ion temperature and density profiles used in the simulations are listed in table 2. In each case n_0 and T_0 are the central bulk ion density and temperature respectively, n_1 and T_1 denote the edge density and temperature, and Ψ_1 is the poloidal flux at the magnetic axis. The exponential factor in the density profiles of models 4-6 is prompted by the well-known result that the bulk ion density on a flux surface that is rotating rigidly in the toroidal direction varies as [14]

$$n_i \sim \exp\left[\frac{m_i \Omega^2 R^2}{2(T_i + T_e)}\right]. \tag{25}$$

We assume that $T_i = T_e \equiv T$: in the density profiles of models 4-6, T is given by the corresponding temperature profile in the second column of table 2. The chosen dependence on Ψ of the model profiles in table 2 is motivated primarily by Thomson scattering measurements of electron temperature and density in MAST plasmas with co-current and counter-current NBI [2]. In discharges with co-current NBI, which have relatively low rotation rates, the density profile is typically rather broad while the temperature profile is strongly peaked at the magnetic axis. In contrast, discharges with counter-current NBI, and high (counter-current) rotation rates, tend to have peaked density profiles and broader temperature profiles. Although the various models listed in table 2 are thus appropriate for different rotation scenarios, we have carried out simulations for every combination of profile model and rotation frequency, in order to separate effects arising purely due to rotation from those associated with the choice of profile. It should be noted that in models 4-6 the parameter n_1 is only equal to the bulk ion edge density at $R = R_0$.

3.3. MAST simulation results

In each simulation the orbits of 10^4 impurity ions, initially at rest at the magnetic axis ($R = R_0$) were computed for at least one confinement time (determined by the period taken for the number of confined ions to fall to $1/e$ of its initial value). Table 3 gives the confinement time obtained using `CUEBIT` for each model and rotation scenario.

There is a strong dependence of confinement time on the temperature and density profiles of the bulk plasma: broadening the temperature profile for a given rotation scenario significantly increases the confinement time, while a broadening of the density profile generally degrades the confinement. Qualitatively, this trend is easily understood: since the central and edge temperatures are fixed, a broadening of the temperature profile makes the plasma on average less collisional, and hence increases

Table 1: Basic parameters used in MAST simulations

Quantity	Description	Value	Units
R_0	major radius	0.964	m
Ψ_0	flux normalisation constant	0.9	Tm^{-2}
γ	plasma elongation constant	0.8	-
R_b	positive constant	0.93	m
Z	test particle charge state	6	-
Δt	timestep normalised to Larmor period	0.1	-
$\log\Lambda$	Coulomb logarithm	15	-
n_0	central bulk ion density	5×10^{19}	m^{-3}
n_1	edge bulk ion density	10^{19}	m^{-3}
T_0	central bulk ion temperature	1	keV
T_1	edge bulk ion temperature	0.1	keV

Table 2: MAST bulk ion temperature/density profiles

Model No.	Temperature profile	Density profile
1	$T_0\left(\Psi/\Psi_1\right)+T_1$	$n_0\left(\Psi/\Psi_1\right)+n_1$
2	$T_0\left(\Psi/\Psi_1\right)+T_1$	$n_0\left(\Psi/\Psi_1\right)^{1/2}+n_1$
3	$T_0\left(\Psi/\Psi_1\right)^{1/2}+T_1$	$n_0\left(\Psi/\Psi_1\right)+n_1$
4	$T_0\left(\Psi/\Psi_1\right)+T_1$	$\left[n_0\left(\Psi/\Psi_1\right)+n_1\right]\exp\left\{m_i\Omega^2(R^2-R_0^2)/4T\right\}$
5	$T_0\left(\Psi/\Psi_1\right)+T_1$	$\left[n_0\left(\Psi/\Psi_1\right)^{1/2}+n_1\right]\exp\left\{m_i\Omega^2(R^2-R_0^2)/4T\right\}$
6	$T_0\left(\Psi/\Psi_1\right)^{1/2}+T_1$	$\left[n_0\left(\Psi/\Psi_1\right)^{1/2}+n_1\right]\exp\left\{(m_i\Omega^2(R^2-R_0^2)/4T\right\}$

Table 3: Computed confinement time of trace C^{6+} ions in MAST (ms)

Model No.	Stationary	Counter-rotating	Co-rotating
1	216.4	101.3	86.8
2	163.3	61.3	50.5
3	318.4	150.5	116.4
4	216.4	64.3	51.8
5	163.3	63.3	49.8
6	223.0	127.5	94.4

the classical confinement time. A broadening of the density profile has the opposite effect.

For every profile model, the impurity ions are optimally confined when the plasma

is non-rotating and least well-confined when it is co-rotating. The reduction in confinement in the rotating cases could be due either to the deconfining effect of centrifugal and $\mathbf{E} \times \mathbf{B}$ drifts, or an increase in neoclassical transport arising from the fact that the ions are displaced outward by the centrifugal force, encounter a lower magnetic field on average, and are thus subject to a higher neoclassical diffusion rate since this scales as ρ^2 [11]. To determine which of these mechanisms plays the dominant role, we plot in figure 4 the final positions of the ions inside the plasma in (R, Z) space for the cases (a) $\Omega = 0$, (b) $\Omega = 2 \times 10^5$ rad s^{-1} and (c) $\Omega = -2 \times 10^5$ rad s^{-1}, using profile model number 1. The black curves tracing out sectors of the plasma boundary indicate the poloidal locations at which ions are lost from the system.

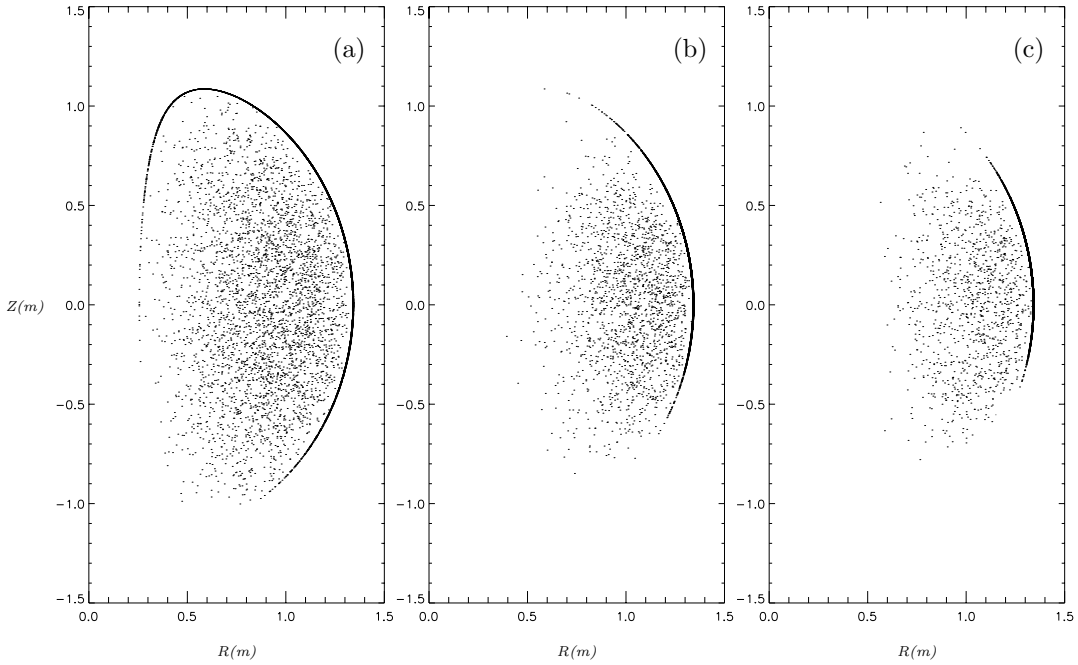

Figure 4: Distribution of impurity ions in (R, Z) plane for (a) $\Omega = 0$, (b) $\Omega = 2 \times 10^5$ and (c) $\Omega = -2 \times 10^5$ rad s^{-1}.

Comparing these plots, it is clear that the ions are indeed strongly displaced outboard by the net effect of the centrifugal force and the R-component of the electric field (as discussed earlier, the latter offsets the former to some extent). In the counter-rotating case all of the impurity ion losses occur outboard of the magnetic axis; this is also true in the co-rotating case, with the losses concentrated in an even narrower range of poloidal angles. The fact that losses occur both above and below the midplane suggests that the confinement degradation in the rotating cases is due mainly to an enhancement in neoclassical transport, rather than being due to centrifugal and electric field modifications to the drift velocity, although in all cases there is a significant up-down asymmetry, suggesting that drifts are playing some role: most losses occur above the midplane, and all the vertical drifts (grad-B, curvature, centrifugal and $\mathbf{E} \times \mathbf{B}$)

are in the positive Z-direction. Reversing the sign of B_φ, we find in each scenario that the poloidal distribution of losses is an almost exact reflection in the midplane of that obtained in the $B_\varphi > 0$ case.

Another striking feature of the results listed in table 3 is that confinement invariably deteriorates when, everything else being equal, the sign of rotation is changed from counter-current to co-current. This appears to be in qualitative agreement with visible bremsstrahlung data from rotating MAST plasmas [2], showing strong central peaking of effective charge ($Z_{\rm eff}$) in the counter-rotating case, and also with much earlier experiments in the ORMAK [32] and PLT [33] tokamaks, indicating that a reversal in the direction of beam injection from co-current to counter-current, for a given level of beam power $P_{\rm NBI}$, produced a higher flux of impurity radiation. Burrell *et al* [34] proposed that this result can be explained by effects arising purely from rotation, rather than the direct collisional interaction of impurity ions with the beam (we take the former but not the latter into account in our simulations). Specifically, Burrell *et al* extended neoclassical theory to include the effects of inertial terms in the impurity ion momentum balance, which are important whenever the rotation velocity is comparable to or greater than the minority ion thermal speed, and found that co-rotation produces an outward radial particle flux while counter-rotation produces an influx.

It should be noted that the absolute rotation rates of counter-injected NBI plasmas generally differ from those of co-injected plasmas with the same $P_{\rm NBI}$, and the plasma profiles are also dissimilar. Moreover the impurity sources tend to be different in the two injection scenarios, due to the fact that counter-injected ions are more likely to be lost promptly and cause sputtering from plasma-facing components [2]. Particular care is therefore required when comparing theory with experiment in this case. The results in table 3 are consistent with the analysis in [34] insofar as they show that impurity ions undergoing purely collisional transport in co-rotating plasmas are significantly less well-confined than those in counter-rotating plasmas. However, in deriving their result Burrell *et al* assumed large aspect ratio, circular cross-section geometry, subsonic rotation, and high (Pfirsch-Schlüter) impurity ion collisionality: none of these assumptions apply throughout the plasma in the simulations reported in this paper.

It is also of interest to examine the dependence of the confinement time on the impurity ion charge state. The appearance of Z in the exponent on the right hand side of equation (6) indicates that the inboard-outboard asymmetry in the minority ion density is greatest for low charge states. In view of the transport enhancement mechanism identified by Helander [11], this suggests that singly-ionised carbon ions are likely to be less well-confined than C^{6+} ions in rotating plasmas. To test this hypothesis, we ran simulations similar to those carried out previously, utilising the same density and temperature profiles, but for singly-ionised rather than fully-ionised carbon ions. We used two of the previously-introduced models for temperature and density, namely models 1 and 5: the results are shown in table 4. It can be seen that the difference in confinement time between counter- and co-rotation is considerably more pronounced for

C^+ ions than it is for fully-ionised carbon ions, with counter-rotation confining the ions for a time approaching almost double that of the co-rotation case. It is also interesting to note that changing the density/temperature profiles seems to have much less of an effect on singly-ionised ions than fully-ionised ones, particularly in the stationary and co-rotating cases.

Table 4: Confinement times of singly- and fully-ionised carbon ions (ms)

Model No.	Z	Stationary	Counter-rotating	Co-rotating
1	1	90.9	64.3	36.4
1	6	216.4	101.3	86.8
5	1	90.1	57.2	35.4
5	6	163.3	83.3	66.2

The reduction in confinement time brought about by changing Z from 6 to 1 is similar in the stationary and co-rotating cases, and greater than that found in the counter-rotating scenario. This suggests that the Z-dependence of the inboard/outboard impurity ion density asymmetry in a rotating plasma, given by equation (6), has little effect on confinement. Since both ρ^2 and τ scale as $1/Z^2$, the classical particle diffusivity given by (15) is independent of Z. However, whereas fully-ionised carbon ions are in the Pfirsch-Schlüter or plateau regimes across the greater part of the plasma in our simulations, C^+ ions are generally in the banana regime since they have a much lower collision frequency. For these ions the neoclassical enhancement of $D_\perp$ above the classical value is much greater than it is for C^{6+}; this appears to account for the reduction in confinement times brought about by replacing $Z = 6$ with $Z = 1$. In practice, given that the ionisation potential of C^+ is around 24 eV, such ions are unlikely to exist in this ionisation state for long in MAST plasmas with core temperatures of around 1 keV.

So far we have considered only the case in which the toroidal rotation speed is approximately equal to the local sound speed of the plasma, i.e. $M \sim \mathcal{O}(1)$. It is useful to consider also the case of subsonic rotation, so that the sensitivity of the results to M can be assessed. Table 5 lists computed confinement times for profile models 1 and 5 when the toroidal Mach number at the magnetic axis is 0.1; for comparison, the corresponding results obtained for stationary plasmas are also listed. As expected, reducing the toroidal rotation velocity of the plasma increases the confinement time of the carbon impurity ions, as centrifugal effects become less important. In this case the rotation causes only a very modest degradation in confinement and there is no significant difference between the results for counter- and co-rotation. This is to be expected if the dominant reason for the increase in transport in the rotating case is that identified by Helander [11], namely the peaking of impurity ion density on the low field side of the tokamak: for the case of fully ionised carbon in a deuterium plasma with $T_e = T_i = T_Z$ the argument of the exponential factor producing the density peaking is equal to $3M^2$ [cf. equation (6)].

Table 5: Confinement times of C^{6+} ions in plasmas with $M = 0.1$ at $R = R_0$ (ms)

Model no.	Stationary	Counter-rotating	Co-rotating
1	216.4	211.1	212.1
5	163.3	161.6	158.4

4. Conclusions and discussion

We have employed a full orbit test-particle code to investigate the collisional transport of carbon impurity ions in ST (MAST-like) plasmas with transonic and subsonic toroidal flows, both counter-current and co-current. The code has been benchmarked by using it to simulate test-particle transport in a very large aspect ratio tokamak with a uniform collision time; in the appropriate limit, the results obtained are in exact agreement with those predicted on the basis of classical transport. In the ST case we have demonstrated that counter-current transonic rotation causes a substantial reduction (by a factor of two or more) in the collisional confinement time of the carbon ions; subsonic rotation has been shown to cause only a slight drop in the confinement time. This behaviour can be attributed principally to the fact that the collisional diffusivity of impurity ions exceeds its flux surface-averaged value, the reason for this being that the ions are displaced outward from the tokamak symmetry axis by the net effect of centrifugal and electric field forces [11]. For a range of temperature and density profile models, we have shown that reversing the direction of rotation from counter-current to co-current causes a further significant reduction in the confinement time. Reducing the charge state of the carbon ions from 6 to 1 also causes a large drop in the confinement time, although this appears to be due mainly to the relatively low collisionality of C^+ ions rather than any effect associated specifically with rotation. In every case we have studied, there is an up/down asymmetry in the losses that reflects the direction of the net vertical drift of the impurity ions.

Our results indicate that the removal of impurity ions is favoured by the use of co-current (rather than counter-current) NBI, as suggested by neoclassical theory in the large aspect ratio, Pfirsch-Schlüter, subsonic limit [34] and by measurements of impurity radiation from several past and present tokamaks [2, 32, 33]. We stress, however, that care should be taken to avoid simplistic comparisons with experimental data. Apart from the differences, noted previously, in the rotation rates, profiles and impurity sputtering rates of plasmas heated by co-NBI and counter-NBI, there is the important caveat that, except in the vicinity of transport barriers, impurity ions undergo turbulent as well as collisional transport. Indeed, the fact that relatively long energy confinement times have been achieved in MAST discharges with transonic counter-rotation [2] despite a predicted enhancement in neoclassical transport [11] illustrates the importance of non-collisional processes in determining tokamak plasma confinement. Notwithstanding the difficulties of making contact with experimental data, our results show that test-particle simulations have a useful role to play in

illuminating the physics of collisional transport in tokamak plasmas in regimes that are not easily accessible to analytical description. We comment finally that the test-particle simulation method could be extended in a fairly straightforward manner to study trace impurity transport in a plasma with a prescribed spectrum of turbulence, based either on experimental diagnostic information [35] or nonlinear numerical simulations of global tokamak turbulence [36, 37].

Acknowledgments

Helpful conversations with Dr Jack Connor are gratefully acknowledged. This work was supported by the United Kingdom Particle Physics and Astronomy Research Council/Science & Technology Facilities Council (through a CASE studentship), the United Kingdom Engineering and Physical Sciences Research Council, and the European Communities under the Contract of Association between EURATOM and UKAEA. The views and opinions expressed herein do not neccessarily reflect those of the European Commission.

References

[1] Sykes A *et al.* 2001 *Nucl. Fusion* **41** 1423

[2] Akers R J *et al* 2005 *Proc. 20th IAEA Fusion Energy Conference* (Vilamoura, Portugal, 2004) paper EX/4-4 (Vienna: IAEA)

[3] Helander P, Akers R J and Eriksson L-G 2005 *Phys. Plasmas* **12** 112503

[4] McClements and Thyagaraja A 2006 *Phys. Plasmas* **13** 042503 (2006)

[5] Thyagaraja A, Schwander F and McClements K G 2007 *Phys. Plasmas* **14** 112504

[6] Chapman I T, Hender T C, Saarelma S, Sharapov S E, Akers R J, Conway N J and the MAST Team 2006 *Nucl. Fusion* **46** 1009

[7] Popov A M *Proceedings of the 33rd EPS Conference on Plasma Physics*, edited by F. De Marco and G. Vlad (European Physical Society, 2006), Vol. **30I**, P-1.106

[8] Liu Y Q *et al.* 2006 *Phys. Plasmas* **13** 056120

[9] Hinton F L and Wong S K 1985 *Phys. Fluids* **28** 3082

[10] Wong S K 1987 *Phys. Fluids* **30** 818

[11] Helander P 1998 *Phys. Plasmas* **5** 1209

[12] Smeulders P 1986 *Nucl. Fusion* **26** 267

[13] Alper B, Edwards A W, Giannella R, Gill R D, Ingesson C, Romanelli M, Wesson J, Zastrow K-D 1996 *23rd EPS Conf. on Controlled Fusion and Plasma Physics (Kiev, Ukraine)* ECA vol 20C part I p.163

[14] Wesson J A 1997 *Nucl. Fusion* **37** 577

[15] Hsu C T and Sigmar D J 1990 *Plasma Phys. Controlled Fusion* **32** 499

[16] Fülöp T and Helander P 1999 *Phys. Plasmas* **6** 3066

[17] Newton S and Helander P 2006 *Phys. Plasmas* **13** 012505

[18] Hamilton B, McClements K G, Fletcher L and Thyagaraja A 2003 *Solar. Phys.* **214** 339

[19] Maschke E K and Perrin H 1980 *Plasma Phys.* **22** 579

[20] Savenko N, McClements K G and Thyagaraja A 2006 *33rd EPS Conf. on Plasma Physics (Rome, Italy)* ECA Vol. 30I P-1.094

[21] Solov'ev L S 1968 *Sov. Phys. JETP* **26** 400

[22] Freidberg J P 1987 *Ideal Magnetohydrodynamics* (New York: Plenum)

[23] Thyagaraja A and McClements K G 2006 *Phys. Plasmas* **13** 062502

[24] Ware A A 1970 *Phys. Rev. Lett.* **25** 15

[25] Helander P, Eriksson L-G, Akers R J, Byrom C, Gimblett C G, and Tournianski M R 2002 *Phys. Rev. Lett.* **89** 235002

[26] Ermak D L, and Buckholz H 1980 *J. Comput. Phys.* **35** 169

[27] Huba J D 2000 *NRL Plasma Formulary* (Washington: Naval Research Laboratory)

[28] Helander P, and Sigmar D J 2002 *Collisional Transport in Magnetized Plasmas* (Cambridge: Cambridge University Press) p 6

[29] Einstein A 1905 *Ann. Phys. (Leipzig)* **17** 549

[30] Fourier J B J 1822 *La Théorie Analytique de la Chaleur* (Paris: Firmin Didot) p 386

[31] Watson G N 1944 *A Treatise on the Theory of Bessel Functions, 2nd Edition* (Cambridge: Cambridge University Press) p 576

[32] Lyon J F, Isler R C, Murakami M, Bush C E, Dunlap J L, Howe H C, Jahns G L, Ketterer H E, Mihalczo J T, Neidigh R V, Paré V K and Wolgen J B 1977 *8th European Conference on Controlled Fusion and Plasma Physics (Prague, Czechoslovakia)* (Prague: Czechoslovak Academy of Sciences) Vol 1, p 23

[33] Suckewer S *et al.* 1981 *Nucl. Fusion* **21** 981

[34] Burrell K H, Ohkawa T and Wong S K 1981 *Phys. Rev. Lett.* **47** 511

[35] Donné A J H, van Gorkom J C, Udintsev V S,1, Domier C W, Krämer-Flecken A, Luhmann N C Jr, Schüller F C and TEXTOR team 2005 *Phys. Rev. Lett.* **94** 085001

[36] Thyagaraja A 2000 *Plasma Phys. Control. Fusion* **42** B255

[37] Idomura Y, Tokuda S and Kishimoto Y 2003 *Nucl. Fusion* **43** 234